Resonant and Nonresonant Electron Cyclotron Heating at Densities above the Plasma Cutoff by O-X-B Mode Conversion at the W7-As Stellarator

H. P. Laqua, V. Erckmann, H. J. Hartfuß, H. Laqua,
W7-AS Team, and ECRH Group*
Max-Planck-Institut für Plasmaphysik, EURATOM Ass., D-85748 Garching, Germany
(Received 25 November 1996)

The extension of the experimentally accessible plasma densities with electron cyclotron heating beyond the plasma cutoff density and the removal of the restriction to a resonant magnetic field, both via mode conversion heating from an O-wave to an X-wave and, finally, to an electron Bernstein (O-X-B) wave, was investigated and successfully demonstrated at the W7-AS stellarator. In addition to the heating effect, clear evidence for both mode conversion steps was detected for the first time. [S0031-9007(97)03011-1]

PACS numbers: 52.50.Gj, 52.35.Hr, 52.35.Mw, 52.55.Hc

Electron cyclotron resonance heating (ECRH) is a very efficient method to heat magnetically confined fusion plasmas. However, the accessible plasma density is limited by a critical density (cutoff density). On the other hand, the prospected large stellarator W7-X will have operational regimes above the cutoff density of the proposed ECRH heating system. A possibility for overcoming the density limit is the O-X-B mode conversion process proposed by Preinhaelter and Kopecký [1] in 1973. This process is a general physics phenomenon of EC waves propagating in hot magnetized plasmas, such as ionospheric or fusion plasmas. Here O, X, and B represent the ordinary, extraordinary, and electrostatic mode, the so-called electron Bernstein mode. The essential part of this scheme is the conversion of the O-wave launched by an antenna from the low field side into an X-wave at the O-wave cutoff layer. This mode conversion requires an O-wave oblique launch near an optimal angle. As shown in Fig. 1 the transverse refractive indices N_x of the O-wave and X-wave along a wave trajectory in a density gradient are connected at the optimal launch angle with a corresponding longitudinal (parallel B_0) index $N_{z,opt}^2 = [Y/(Y + 1)]$ with $Y = \omega_{ce}/\omega$ (ω is the wave frequency, ω_{ce} is the electron cyclotron frequency) without passing a region of evanescence ($N_x^2 < 0$). For nonoptimal launch an evanescent region always exists near the cutoff surface. The geometrical size of this evanescent region depends on the density scale length $L = n_e/(\partial n_e/\partial x)$, and a considerable fraction of the energy flux can be transmitted through this region, if L becomes small. The power transmission function $T(N_y, N_z)$ is [2]

$$T(N_y, N_z) = \exp\left\{ -\pi k_0 L \sqrt{\frac{Y}{2}} [2(1 + Y) \times (N_{z,opt} - N_z)^2 + N_y^2] \right\},$$

where N_y and N_z are the poloidal and longitudinal components of the vacuum refractive index and k_0 is the wave number. This angular dependence (N_z dependence) was used, among other criteria, in the experiments to identify the O-X conversion process. After the O-X conversion the X-wave propagates back to the upper hybrid resonance (UHR) layer where the electron Bernstein branch of the dispersion relation is connected to the X-mode branch in the hot plasma approach as shown in Fig. 1, and a complete conversion into electron Bernstein waves (EBW) takes place. For EBW's a density limit does not exist, and they can propagate towards the plasma center, where they are absorbed near the electron cyclotron resonance layer or, in the nonresonant case, by collisional multiple pass damping.

Ray tracing calculations were performed in order to get a more detailed insight into the O-X-B scheme. Density, temperature, and magnetic field profiles similar to that of a typical neutral beam sustained W7-AS plasma were used for model calculations in a straight plasma cylinder. We use the nonrelativistic hot dielectric tensor with a correction for electron ion collisions given by [3] and an isotropic electron temperature. The ray trajectory in the x-z plane is shown in Fig. 2. The beam is launched

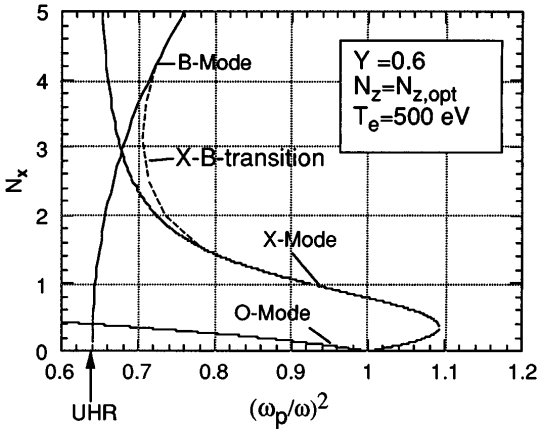

FIG. 1. Refractive index N_x versus ω_p^2/ω^2 for the O-X-B conversion process. The transition represents the connection of the X mode and the B mode due to the hot dielectric tensor.

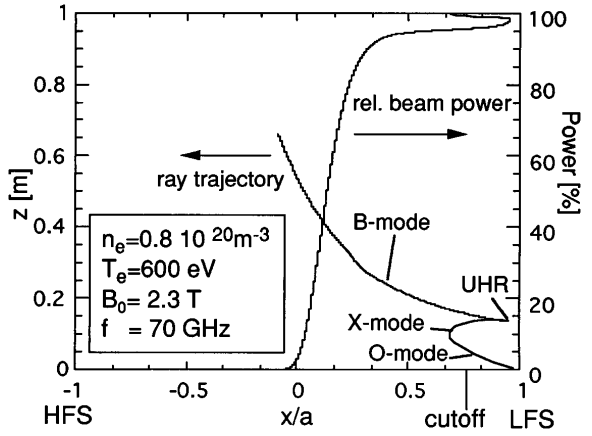

FIG. 2. Calculated ray trajectory in the x-z plane and relative beam power for resonant O-X-B heating as a function of the x coordinate.

from the low field side and propagates through the cutoff, where it is converted into an X-mode. Then it moves back to the UHR layer, where the X-B conversion takes place. The EBW's are absorbed near the cyclotron resonance at the plasma center. A small fraction of the beam power is lost at the UHR due to finite plasma conductivity. The power deposition zone for resonant heating strongly depends on the magnetic field and the electron temperature. EBW's experience a cutoff layer ($N \rightarrow 0$) at the upper hybrid resonance surface (see Fig. 1), which in the nonresonant or higher harmonic ($\omega_{ce}/\omega < 1$) field totally encloses the inner plasma. The radiation is then trapped inside the plasma like in a hohlraum. The EBW's are either reflected at the UHR surface in the case of an oblique angle of incidence or are backconverted to X waves which are converted again to the EBW's at their next contact with the UHR. Radiation can only escape through the small angular window for O-X and X-O conversion, respectively. In the absence of an electron cyclotron resonance in the plasma the EBW's may be absorbed due to finite plasma conductivity after some reflections at the UHR layer. In calculations for the nonresonant case more than 40% of the beam power is absorbed due to finite plasma conductivity after six passes through the plasma.

In the consideration hitherto existing, the conversion layer was assumed to be smooth; in reality it is rough and wavy due to density fluctuations. This introduces an effective beam divergence much higher than the intrinsic one and can reduce the O-X conversion efficiency considerably. With a statistic description of the cutoff surface roughness (only fluctuations with a wave vector in the poloidal direction were considered), the probability density function of the poloidal component N_y (similar to a poloidal beam divergence),

$$p(N_y) = \frac{\lambda_y}{\sqrt{2\pi}\,\sigma_x}\,\exp\left(-\frac{N_y^2\lambda_y^2}{(1-N_y^2)2\sigma_x^2}\right)(1-N_y^2)^{-3/2},$$

could be calculated as a function of the fluctuation amplitude standard deviation $\sigma_x = L\tilde{n}_e/n_e$ ($\tilde{n}_e/n_e$ is the relative fluctuation amplitude) and the poloidal correlation length λ_y. The modified power transmission function T_{mod} (O-X conversion efficiency) is then

$$T_{\mathrm{mod}}(N_z) = \int_{-1}^{1} T(N_z, N_y)p(N_y)dN_y\,.$$

In Fig. 3 the modified transmission is calculated as a function of the parameter k_0L for five different relative density fluctuation amplitudes. In all calculations the poloidal correlation length was assumed to be 2 cm. It can be clearly seen that a significant heating efficiency is obtained only at a very small density scale length or a very low fluctuation amplitude.

In the X-B conversion process near the UHR parametric instabilities (PI) are expected [4,5], which generate decay waves with frequencies of the incident pump wave ω plus and minus the harmonics of the lower hybrid frequency ω_{LH} and the lower hybrid (LH) wave itself [6]. Their appearance is an evidence that X-B conversion occurs.

Experimental results.—The experiments were performed at the W7-AS stellarator (major radius $R = 2.0$ m, minor radius $a = 0.18$ m) with two 70 GHz gyrotrons with 110 kW power each. A detailed description of W7-AS and its 70 GHz ECRH system can be found in [7]. The central magnetic field was set between 1.25 and 2.0 T and the edge rotational transform ι, taken from the magnetic reconstruction, near 0.35 according to the experimental requirements. The central density of the neutral beam injection (NBI) sustained target plasma was up to 1.6×10^{20} m^{-3}, which is more than twice the 70 GHz O-mode cutoff density. Co- and counter-NBI, with 380 kW power each, were used to compensate the momentum transfer to the plasma.

(1) *Variation of the edge rotational transform.*—The edge turbulence level can be changed at W7-AS by the

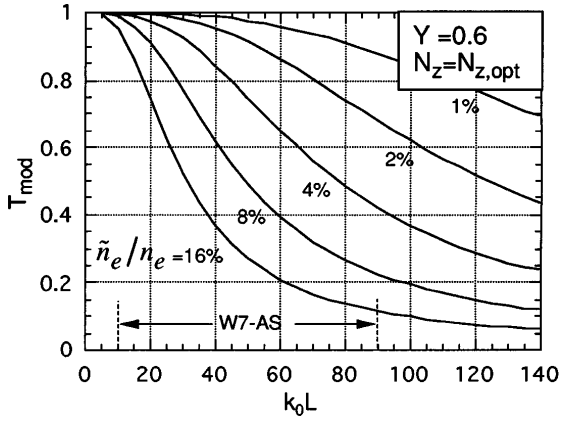

FIG. 3. Modified O-X conversion in the presence of density fluctuations at the plasma cutoff layer versus normalized density scale length k_0L for five different relative density fluctuation amplitudes.

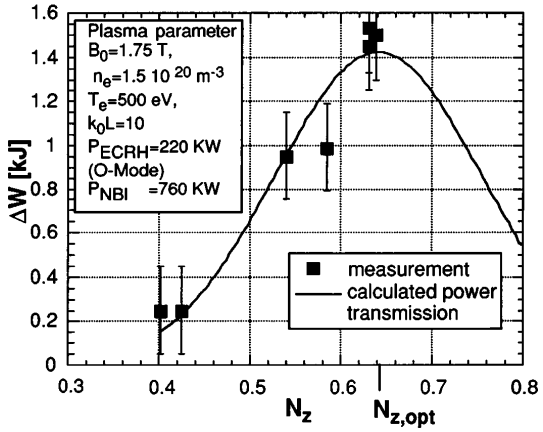

FIG. 4. Increase of the plasma energy content by O-X-B heating versus the longitudinal vacuum refractive index N_z of the incident O wave. The solid line is the calculated transmission function multiplied by the maximum energy increase.

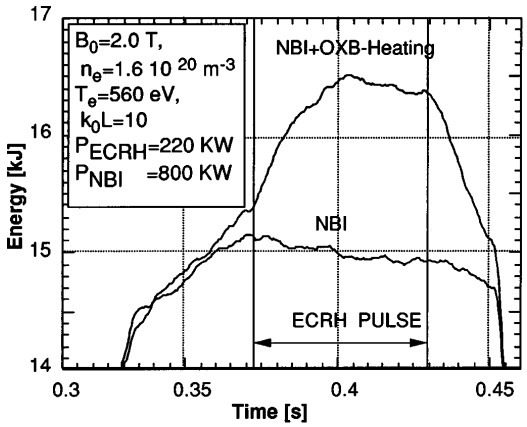

FIG. 5. Energy content (diamagnetic signal) of a NBI discharge with and without nonresonant O-X-B heating.

boundary conditions. This has an influence to the density profile shape and the density fluctuation activity. In order to investigate the influence of both to the O-X conversion efficiency and to proof our statistic model, a scan of the edge rotational transform ι was done. The flexibility of W7–AS allows one to investigate both extreme cases, i.e., target plasmas with $k_0L \leq 10$ and with a relative density fluctuation amplitude of more than 25% or peaked density profiles ($k_0L = 60$) with a relative fluctuation amplitude of less than 2%. For both cases, high conversion efficiencies ($>70\%$) were experimentally measured, while for target plasmas with $k_0L > 30$ and high fluctuation amplitudes ($>20\%$) only low or no O-X-B heating could be achieved as predicted by our statistic model (see Fig. 3).

(2) *Variation of the launch angle.*—The launch angle of the incident O-mode polarized wave was varied at fixed heating power (220 kW) at a nonresonant magnetic field. The increase of the total stored plasma energy (from the diamagnetic signal) depends strongly on the launch angle (see Fig. 4), which is typical for the O-X conversion process, and fits well to the calculation. Here the power transmission function was normalized to the maximum energy increase. The central density was 1.5×10^{20} m^{-3}, which is more than twice the cutoff density; the central electron temperature was 500 eV. Heating at the plasma edge could be excluded since, at the nonresonant magnetic field of 1.75 T, no electron cyclotron resonance existed inside the plasma. Because of the technical limitation of the maximum launch angle, only the left part of the reduced transmission function could be proved experimentally. Nonresonant heating was clearly observed at magnetic fields up to 2.0 T. At the maximum field the plasma energy content increased by about 1.5 kJ compared to a similar discharge with neutral beam injection only as shown in Fig. 5. Two 70 GHz beams in O-mode polarization (110 kW power each) were launched with an angle of 40° with respect to the perpendicular launch into a NBI (760 kW) sustained target plasma with a central density of 1.6×10^{20} m^{-3} and a central temperature of 560 eV. More than 70% of the heating power was found in the plasma if the power scaling of the energy confinement ($P^{-0.6}$) was taken into account. Thus O-X-B heating turned out to be very efficient.

(3) *Density variation and parametric instability.*—In these experiments, it should be demonstrated that a density threshold (O-cutoff) exists for the O-X-B heating process. For this, the plasma was built up by one 70 GHz gyrotron

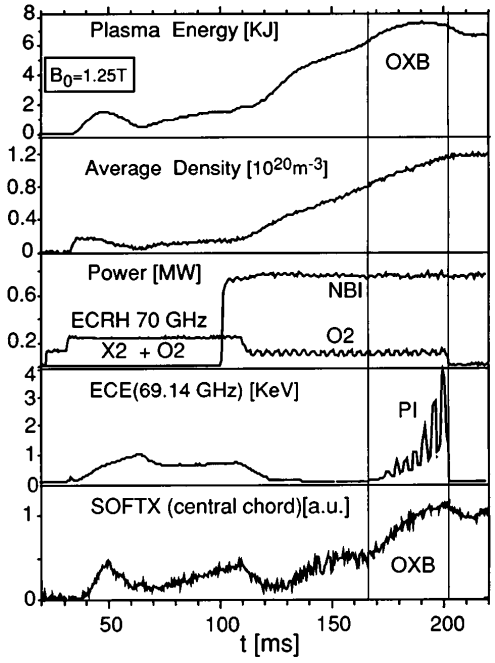

FIG. 6. Temporal development of some plasma parameter during a O-X-B heated discharge. From the top: plasma energy estimated from the diamagnetic signal, average density from the interferometric measurement, heating power, intensity of ECE and PI, and central soft X signal. The markers show the O-X-B-heating interval.

in X polarization in a resonant central magnetic field of 1.25 T. Then the density was slowly ramped up to density above the O-cutoff. In parallel, as shown in Fig. 6, a second 70 GHz beam O-mode polarized with the optimal launch angle and modulated with 20% amplitude was launched into the plasma. During the plasma buildup, thermal EC emission (ECE) was detected. As soon as the cutoff density was reached, ECE vanished and O-X-B heating started, which caused an increase of the plasma energy and central soft-x emission shown in Fig. 6. Simultaneously, the PI at the X-B conversion process generated a decay spectrum, whose high frequency part could be measured with the ECE detector. The modulation amplitude strongly exceeded that of the pump wave, which clearly demonstrated the nonlinear character (power threshold) of the PI. Figure 7 shows the high frequency decay spectrum. Two redshifted lines and one blueshifted line can be recognized. Their spectral distances to the 70 GHz pump wave, which was suppressed by a Notch filter, are multiples of the lower hybrid resonance (LHR) frequency ($\sim$900 MHz). The spectrum of the LHR oscillation itself could be detected by a loop antenna. The LHR oscillation shows a high degree of correlation with the high frequency decay waves.

In conclusion, efficient O-X-B heating with 70 GHz electron cyclotron waves was clearly demonstrated for resonant and nonresonant fields at W7-AS. Both, the angular dependence of the O-X conversion and the parametric instability which is typical for X-B conversion, could be experimentally verified. This is an excellent test of hot plasma wave theory. Density fluctuations at the cutoff layer play a significant role in the O-X conversion process and need to be taken into account. As a consequence of this, for large fusion devices ($k_0 L > 60$), O-X-B heating may become difficult. Here the high confinement regime (H-mode) with its strongly reduced turbulence level and its steepened edge density profile could provide proper conditions for O-X-B heating. With increased gyrotron power and improved measurement techniques of the power deposition profiles, further investigations of the O-X-B heating at W7-AS are envisaged to explore the potential of resonant and nonresonant O-X-B heating for routine high density operation. Besides the application for plasma heating, the O-X-B window may also gain importance for temperature diagnostic of overdense plasmas via electron Bernstein wave emission for fusion physics as well as in ionospheric research.

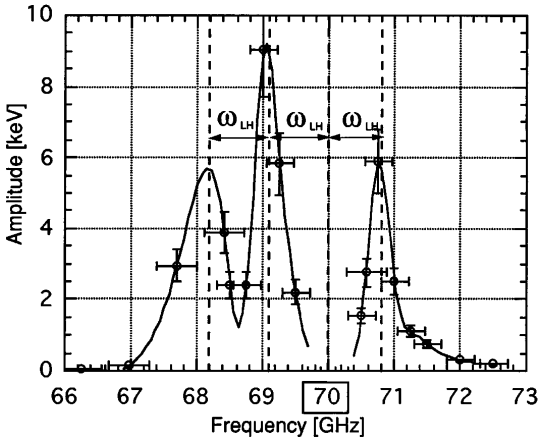

FIG. 7. High frequency spectrum of the parametric decay waves generated in the X-B process. The incident wave frequency is 70 GHz and the LHR frequency is about 900 MHz.

*Permanent address: Institut für Plasmaforschung, Univ. Stuttgart, D-70569 Stuttgart, Germany

[1] J. Preinhaelter and V. Kopecký, J. Plasma Phys. **10**, 1 (1973).
[2] E. Mjølhus, J. Plasma Phys. **31**, 7 (1984).
[3] T. H. Stix, *Theory of Plasma Waves* (McGraw-Hill, New York, 1962).
[4] D. G. Bulyginsky, V. K. Gusev, V. V. Djachenko, M. A. Irzak, M. Yu. Kantor, M. M. Larionov, L. S. Levin, G. A. Serebreny, and N. V. Shustova, in *Proceedings of the 11th European Conference on Controlled Fusion and Plasma Physics, Aachen, 1983* (Pergamon, New York, 1983), Vol. II, p. 457.
[5] R. Wilhelm, V. Erckmann, G. Janzen, W. Kasparek, G. Müller, E. Räuchle, P. G. Schüller, K. Schwörer, and M. Thumm, Plasma Phys. Control. Fusion **26**, No. 12A, 1433–1444 (1984).
[6] D. G. Swanson, *Plasma Waves* (Academic Press, New York, 1989).
[7] H. Renner *et al.*, Plasma Phys. Control. Fusion **31**, No. 10, 1579–1596 (1989).